

## Targeted expression of *shibire<sup>ts</sup>* and *semaphorin 1a* reveals critical periods for synapse formation in the giant fiber of *Drosophila*

R. K. Murphey<sup>1,\*</sup>, Stephan J. Froggett<sup>1</sup>, Phyllis Caruccio<sup>1</sup>, Xiaoliang Shan-Crofts<sup>1</sup>, Toshihiro Kitamoto<sup>2</sup> and Tanja A. Godenschwege<sup>1</sup>

<sup>1</sup>University of Massachusetts, Department of Biology, Morrill Science Center, Amherst, MA 01003, USA

<sup>2</sup>Division of Neurosciences, Beckman Research Institute of the City of Hope, 1450 E. Duarte Road, Duarte, CA 91010, USA

\*Author for correspondence (e-mail: rmurphey@bio.umass.edu)

Accepted 1 May 2003

### SUMMARY

In order to determine the timing of events during the assembly of a neural circuit in *Drosophila* we targeted expression of the temperature-sensitive *shibire* gene to the giant fiber system and then disrupted endocytosis at various times during development. The giant fiber retracted its axon or incipient synapses when endocytosis was blocked at critical times, and we perceived four phases to giant fiber development: an early pathfinding phase, an intermediate phase of synaptogenesis, a late stabilization process and, finally, a mature synapse. By co-expressing

*shibire<sup>ts</sup>* and *semaphorin 1a* we provided evidence that Semaphorin 1a was one of the proteins being regulated by endocytosis and its removal was a necessary part of the program for synaptogenesis. Temporal control of targeted expression of the *semaphorin 1a* gene showed that acute excess Semaphorin 1a had a permanent disruptive effect on synapse formation.

Key words: Synaptogenesis, Semaphorin, Endocytosis, Dynamin, *Drosophila*

### INTRODUCTION

The transformation of a motile growth cone to a sedentary synapse requires a conversion of the cell surface and cytoskeletal components of the growth cone from the requirements for movement to the requirements for synaptic transmission. Although the molecular aspects of this conversion are poorly understood there are a number of suggestions that endocytosis is a critical component of the transformation. Growth cones exhibit considerable membrane trafficking and depend on endocytosis for their activities that include the mechanics of movement and the regulation of receptors by ligand-induced endocytosis (Diefenbach et al., 1999; Fournier et al., 2000; Journey et al., 2002; Kamiguchi and Lemmon, 2000). Recently, receptor and membrane trafficking has emerged as a regulator of a variety of cell-cell interactions and a wide variety of receptors have been demonstrated to be inactivated by ligand-induced endocytosis (Hicke, 1999). Blocking endocytosis with a temperature-sensitive allele of dynamin interferes with this process, disrupting the balance of proteins on the surface of the pre- and postsynaptic cells during synaptogenesis (Heerssen and Segal, 2002).

The complexities of the signaling pathways that regulate synapse formation are only now being recognized. At the *Drosophila* neuromuscular junction, the trafficking of TGF $\beta$  and Wingless/Frazzled have recently been linked to synaptic differentiation. In the case of the TGF $\beta$  the role of membrane trafficking was emphasized because proteins in the endosomal

system affect signaling and their loss led to a large over growth of the presynaptic terminal (Sweeney and Davis, 2002). Similarly Wingless/Frazzled and its trafficking has been linked to maturation of the presynaptic terminal (Packard et al., 2002). In both cases the first step in the process is the dynamin-dependent endocytosis of the receptor. Thus, we reasoned that it might be useful to disrupt endocytosis at various times during the transition from growth cone to synapse and determine whether there are critical periods during which endocytosis is crucial to synapse formation, maturation or stabilization.

In *Drosophila*, there is suggestive evidence that blocking endocytosis during particular stages of development of the giant fiber (GF) system disrupts synaptogenesis (Hummon and Costello, 1987). The original mutation in dynamin was a temperature-sensitive paralytic mutant in *Drosophila* called *shibire*, which was linked to synaptic transmission (Koenig and Ikeda, 1996; van der Bliek and Meyerowitz, 1991) and to the regulation of signaling systems (Di Fiore and De Camilli, 2001). The mutant functions as a dominant negative at the restrictive temperature and can be used to block endocytosis on a wild-type background (Damke et al., 1995a; Damke et al., 1995b; Kim and Wu, 1987). The problem with the original experiments that examined development of the giant fiber system was that temperature shifts blocked endocytosis in all cells and made the interpretation of the results difficult (Hummon and Costello, 1987). The temperature-sensitive allele of *shibire* has now been cloned into a P-element (UAS-*shi<sup>ts</sup>*) and can be targeted to cells of interest in *Drosophila*,

thereby gaining both temporal and cell specific control over endocytosis (Kitamoto, 2002). In addition, a panel of *Gal4* gene targeting constructs for the GF system is available, which allow targeted expression to different components of the GF system (Allen et al., 1998; Allen et al., 1999; Allen et al., 2000; Godenschwege et al., 2002a). This provides a method to assess the required timing for endocytosis in the developing nervous system.

In the present report, we targeted expression of the temperature-sensitive dynamin to the GF system and blocked endocytosis during development. Blockade of endocytosis at different times revealed four phases of sensitivity and temperature shifts during each phase have a different consequence for the development of the GF system. We previously demonstrated that Semaphorin 1a (Sema1a) was involved in assembly of the GF system (Godenschwege et al., 2002a) and we now show that defects were induced primarily during the period of synapse formation. Finally, when UAS-*sema1a* was co-expressed with UAS-*shi<sup>ts</sup>* and endocytosis was blocked at different times, the two effects interacted, suggesting that one of the proteins being regulated by endocytosis was Sema1a.

## MATERIALS AND METHODS

### Fly stocks and rearing methods

Specimens were reared at one of two baseline temperatures 18°C or 22°C. The duration of pupal development was ~144 hours at 22°C and 192 hours at 18°C. When third instar specimens stopped wandering and shorten, this was considered the onset of metamorphosis and all timing refers to this as P0 or time 0. We used the number of hours for staging the pupae rather than the embryonic markers of (Bainbridge and Bownes, 1981) because most of the events occur in a time period when there were relatively few markers. The variance in developmental timing had a number of components, including intrinsic developmental variation between different strains and the variance of the rate of growth of the GF. As assayed by time to emergence the overall variance was between 10 and 15% of the duration of the pupal stage. Pupae were collected at P0 and moved to separate vials for treatment. For temperature shift experiments, we moved vials containing selected pupae into an incubator at the restrictive (usually 30°C) temperature (Koenig and Ikeda, 1996). The specimens were temperature shifted for 24 hours unless otherwise specified. The 24-hour temperature shift represents 12.5% of development for specimens reared at 18°C and 16.6% of pupal development for specimens reared at 22°C.

Three P[Gal4] drivers were used to drive various constructs in the GF system. The enhancer known as P[Gal4]-A307 an insert on the second chromosome (Allen et al., 1998) was expressed primarily in the GF and weakly in other components of the system including the tergotrochanteral motoneuron (TTMn) and the dorsal longitudinal motoneuron (DLMn) and the muscles of the thorax particularly the tergotrochanteral muscle (TTM) and the dorsal longitudinal muscle (DLM). The enhancer known as P[Gal4]-c17 an insert on the second chromosome (Allen et al., 1999; Godenschwege et al., 2002a) is expressed in the GF but not in the postsynaptic neurons and it can be used for exclusively presynaptic expression. Finally, the postsynaptic cells were labeled by the P[shakB-Gal4] construct, a fragment of the gap junction promoter fused to Gal4 and inserted on the 2nd chromosome (Jacobs et al., 2000). This construct is expressed in TTMn, DLMn, a variety of other motoneurons and the PSI (peripherally synapsing interneuron). The UAS-*shi<sup>ts</sup>* on the third chromosome was obtained from Kitamoto and expressed under

control of one of the three Gal4 constructs (Kitamoto, 2001; Kitamoto, 2002). A UAS-*sema1a* construct on the 2nd chromosome was used to express Sema1a (Yu et al., 1998). Finally, a UAS-*lacZ* construct on either chromosome 1, 2 or 3 was expressed under control of the relevant enhancer and expression revealed immunohistochemically.

### Blocking endocytosis

Endocytosis was compromised by shifting specimens to the restrictive temperature (30°C in most experiments). Although development speeds up with temperature it shows a biphasic curve and slows at 30°C to a rate similar to that at 22°C (Ashburner, 1989) so this temperature shift has relatively small effect on the rate of development. To show that the construct was blocking endocytosis, we expressed UAS-*shi<sup>ts</sup>* in the motoneurons under the control of A307 and then temperature shifted the specimens acutely. We mounted the specimens on wax on a peltier battery which allowed a rapid shift of temperature (less than 3 minutes) from 22°C to 30°C. Recordings were obtained before during and after the temperature shift. This blocked synaptic transmission within minutes at the DLM, in a manner parallel to that seen in early experiments on the original *shibire* mutant (Koenig and Ikeda, 1996), and at the TTM.

### Physiology

The physiological methods are standard (Oh et al., 1994; Tanouye and Wyman, 1980) and we have modified them only slightly (Allen et al., 1999; Godenschwege et al., 2002b). The specimens were anesthetized by placing them on ice and then mounted on soft wax. Tungsten electrodes were used to stimulate the GF, and glass electrodes to record from the muscles. The data was recorded using P-Clamp software (Axon Instruments).

In specimens (A307/+;UAS-*shi<sup>ts</sup>*/+) reared at 22°C and never given any form of temperature shift, we were unable to obtain recordings from the TTM. Sections of the thorax demonstrated that the TTM muscle was small or absent in these specimens although the DLM was normal. The A307 construct is known to be expressed in the muscles of the thorax and we assume that the expression of the P[UAS-*shi<sup>ts</sup>*] in the muscle at 22°C, throughout development disrupts normal muscle development, suggesting that *shi<sup>ts</sup>* has an effect at the non-restrictive temperature. When A307; UAS-*shi<sup>ts</sup>* was reared at 18°C the TTM muscles of control specimens were intact and we used this rearing temperature for the physiological experiments described below. We examined the anatomy of the GFs at both rearing temperatures and in spite of the absence of TTM muscles at 22°C and their presence at 18°C we saw no difference in the anatomical phenotypes of the GFs after temperature shifts.

### Immunohistochemistry

The CNS was dissected from adults or pupae at the appropriate stage and standard methods were used to reveal *lacZ* in the various neurons (Allen et al., 1999; Godenschwege et al., 2002b).

### Image processing

Images of selected whole mounted specimens were captured using a SPOT digital camera (Diagnostic Instruments, Sterling Heights MI) and imported into Adobe Photoshop 5.0 software. Montages were constructed using the clone tool to show a two-dimensional image of the three dimensional neurons.

## RESULTS

### Development of the GF system

The giant fiber (GF) system of the fly consists of a large interneuron that controls the visually evoked escape behavior through its synaptic contacts with thoracic motoneurons

(Tanouye and Wyman, 1980; Thomas and Wyman, 1984; Trimarchi and Schneiderman, 1995). Anatomical studies have provided the outlines of the development of this circuit, summarized schematically in Fig. 1A (Allen et al., 1998; Phelan et al., 1996). The dendrites of the jump motoneuron (TTMn) grow into the target area at the beginning of pupal development, before the axon of the GF reaches the thorax (Jacobs et al., 2000). The GF initiates growth in the late larval stage and the axon leaves the brain and reaches the target area in the second thoracic neuromere by ~25% of pupal development (Allen et al., 1998; Phelan et al., 1996). The growth cone of the GF appears to contact the TTMn dendritic growth cone at this time, and during a synaptogenic phase (~25-50% of pupal time) the GF elaborates a lateral 'bend' along the TTMn that becomes the presynaptic terminal and by 40% of pupal development the two neurons are dye-coupled (Allen et al., 1998; Jacobs et al., 2000; Phelan et al., 1996).

A number of Gal4 constructs are available that target gene expression to the GF system during pupal development. An enhancer trap known as P[Gal4]-A307 (referred to throughout as A307) is expressed strongly in the GF throughout the pupal and adult stages and it is also expressed weakly in some of the targets (Fig. 1B3), including the TTMn during the mid-pupal

stages (Allen et al., 1998; Phelan et al., 1996). The P[Gal4]-c17 enhancer (referred to as c17) is active in the presynaptic GF but not in the postsynaptic motoneurons (Fig. 1B4) and is expressed most strongly just prior to synapse formation and continues expression until emergence of the adult (Allen et al., 2000). The *shakB*(lethal)-Gal4 construct (hereafter called *shakB*) is expressed in the motoneurons particularly the TTMn (Fig. 1B2), during pupal development and expression ceases shortly after emergence of the adult (Jacobs et al., 2000).

The dye injection results provided a very detailed picture of the neurons but rather little about the temporal variability of these developmental processes. By combining the c17 enhancer and the *shakB*-Gal4 element, we labeled the pre- and postsynaptic cells simultaneously and this provided an indication of the variability in GF growth. We focused on the period when the GF was reaching the target area and collected a number of specimens at this time. The results showed that at 33% of pupal development the TTMn dendrite had always reached the midline but there was considerable variability in the position of the GF axon terminal; approximately half (16/33) of the GFs had contacted the TTMn and half had not. In a typical specimen at this stage, both GFs can be seen adjacent to the midline glia but only one has reached the dendrite of the TTMn (Fig. 1B1).

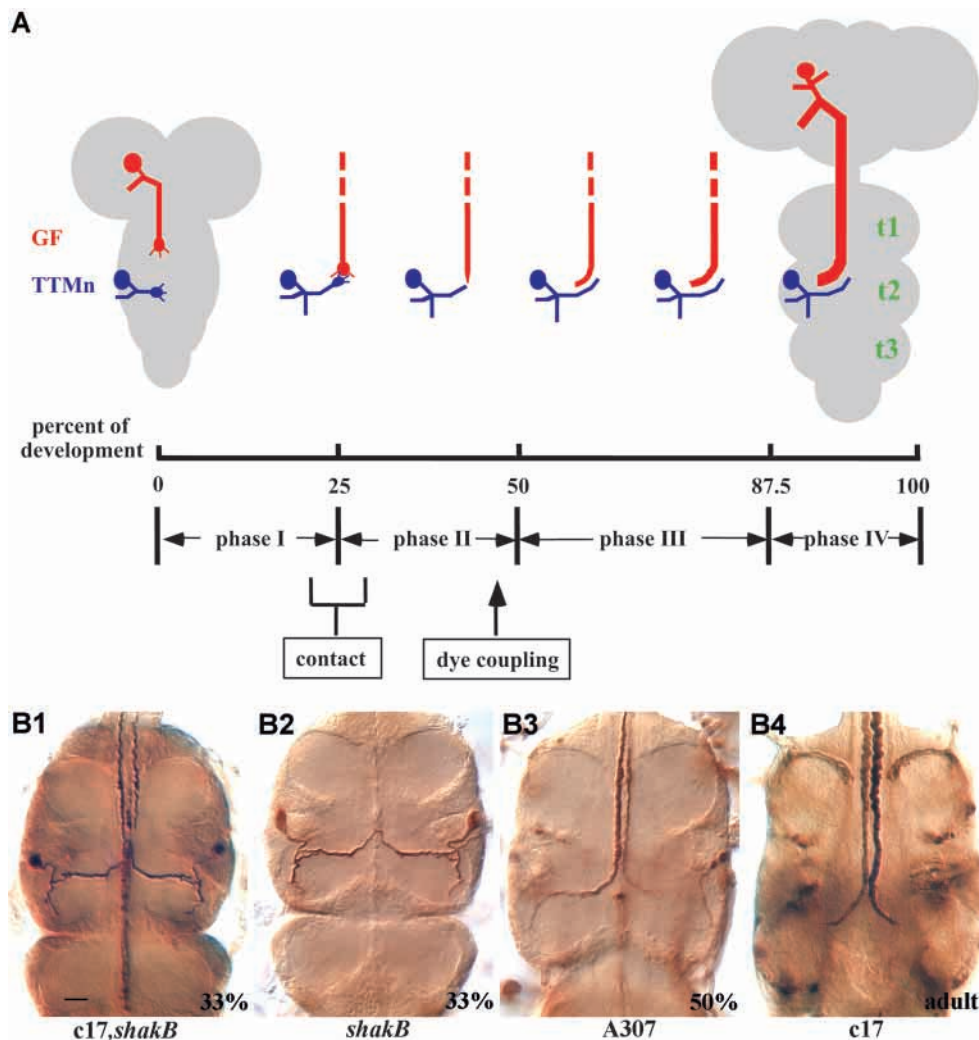


**Fig. 1.** Development of the GF system. (A) GF development. The timing of events is based on the work presented in the present paper as well as the dye injection work of Jacobs et al. (Jacobs et al., 2000). The time line is recorded as percent of pupal development with time zero according to Bainbridge and Bounds (Bainbridge and Bounds, 1981). The phases indicated below the time line were determined experimentally in the present work. The time of dye coupling was determined by Jacobs et al. (Jacobs et al., 2000). t1, t2 and t3: first, second and third thoracic neuromere. (B) Expression patterns of the three Gal4 constructs. (B1) Simultaneous staining of the GF (with c17) and the TTMn (with *shakB*-Gal4) at 33% of pupal development. In this particular specimen, the left GF has reached the TTMn and the right GF has not. (B2) When driven by *shakB*-Gal4, *lacZ* is expressed in the postsynaptic motoneurons and TTMn exhibits the strongest staining. (B3) The P[Gal4]-a307 enhancer is expressed strongly in the GF and more weakly in the postsynaptic cells. In this specimen both GFs are labeled and the dendrites of the left TTMn are revealed. (B4) The P[Gal4]-c17 enhancer is expressed in the GF but not in the motoneurons. The developmental stage of each specimen is indicated in the lower right of each panel. Scale bar: 20  $\mu$ m.

### Blocking endocytosis at different times produces three distinct axonal phenotypes

In order to begin to assess the role of endocytosis in the GF and provide an outline of critical periods in pupal development we blocked endocytosis during various phases and assessed GF structure and function. The P[UAS-*shi<sup>ts</sup>*] (Kitamoto, 2001; Kitamoto, 2002) was expressed under control of the A307 (Fig. 1). We used the A307 because it was expressed strongly in the GF throughout the pupal stages and this allowed us to compromise endocytosis at anytime during pupal development and assess the effects on GF growth. Endocytosis was compromised by shifting specimens from the permissive temperature (18°C or 22°C) to the restrictive temperature (30°C) at various times during pupal development. The restrictive temperature disrupted the pupal development of the GF system and the phenotype in the adult correlated with the timing of the temperature shift. In parallel physiological experiments, we examined the efficacy of the synaptic connections from GFs to the motoneurons by stimulating the GF in the brain and recording from the TTM and DLM muscles in adults (Allen et al., 1999; Tanouye and Wyman, 1980; Thomas and Wyman, 1984). Here, we focus on the monosynaptic GF-TTMn response and use the response of the polysynaptic GF-DLM pathway to determine the percentage of GFs making a connection, demonstrating their presence in the target area. Four phases of sensitivity during development of the GF system were identified. For narrative purposes, we describe these phases as having distinct boundaries although there are continuous transitions between the stages (Tables 1, 2).

#### Phase I (pathfinding)

When the temperature shift was initiated during the first quarter of pupal development (P0-25%) and the GF was examined in the adult stage an unusual overgrowth of the axons was observed in the thoracic neuromeres. In the majority of specimens (61%) the axons branched throughout the second and third neuromeres (Fig. 2A1 and Table 1). In a minority, the GFs grew straight through the target region and terminated in the third thoracic neuromere and a few axons terminated in the subesophageal neuromere in the brain. Correlated with this anatomy, 60% of the GFs reached the target area and were

connected to the DLM (Table 1). The GFs that were able to drive the DLMn did so much less reliably than controls and typically only a single response occurred at the beginning of a train of ten stimuli (Fig. 2B1, Table 1). Unfortunately, the monosynaptic GF-to-TTMn synapse could not be studied during this phase because shifts to the restrictive temperature before 50% of pupal development caused loss or dramatic shrinkage of the TTM muscle fibers, presumably owing to expression by A307 in the muscles (see Materials and Methods).

#### Phase II (target recognition and synapse formation)

When the temperature shift occurred during the period of target recognition and synapse initiation (25-50% of pupal development), the adult axon usually terminated in the target area but the ending was abnormal (Tables 1, 2). Most GF axons lacked the large laterally directed presynaptic terminal (Fig. 2A2). This *bendless*-like phenotype was similar to the original *bendless* mutant phenotype (Thomas and Wyman, 1984; Oh et al., 1994). In accordance with the anatomy, almost all GFs were connected in the target area (either to the DLMn or the TTMn) but the GF-TTMn connection was severely disrupted. The GF-TTMn response was either absent (67%, Table 1) or weakened, as indicated by an increased response latency and the inability to follow stimuli at 100 Hz (Fig. 2B2, Table 1). The defect/absence in the response was attributed to a disruption of the GF-TTMn synapse itself as the direct stimulation of the motoneurons confirmed that the muscle and neuromuscular junction were intact (data not shown). Interestingly, temperature shifts between 17 and 50% (Tables 1, 2) of pupal development occasionally resulted in adult specimens with GFs terminals that can be seen in the brain (Fig. 2A1). No such phenotype was found in control specimens, suggesting that temperature shifts at this pupal developmental stage caused some GFs to retract into the brain and not regenerate after the temperature shift.

#### Phase III (stabilization)

Temperature shifts at 62.5 or 75% of pupal development had minor effects on the GF anatomical phenotype; typically the bend was present and normal in size although it may contain

**Table 1. Critical periods in GF development**

Phase	Stage <sup>†</sup> TS begins	n	Anatomy*				n	Physiology*				
			Wild type (%)	Over- growth (%)	Bendless (%)	Brain (%)		TTM wild type <sup>‡</sup> (%)	TTM latency in ms	TTM FF (%)	TTM dis- connection (%)	TTM or DLM connection (%)
I	0	36	17	61	22	0	16	nd	nd	nd	nd	60
I	12.5	16	19	62	19	0	10	nd	nd	nd	nd	60
II	25	21	13	7	60	20	10	nd	nd	nd	nd	80
II	50	18	21	0	74	5	12	17	1.56 <sup>§</sup>	44.7 <sup>§</sup>	67	92
III	62.5	12	100	0	0	0	10	0	1.96 <sup>§</sup>	56.8 <sup>§</sup>	20	80
III	75	7	100	0	0	0	10	60	1.26 <sup>§</sup>	83	10	100
IV	87.5	13	100	0	0	0	12	85	1.1	100	15	100
	No TS	12	100	0	0	0	15	53	0.87	100	0	93

\*Genotype: anatomy, UAS-*lacZ*/+;A307/+;UAS-*shi<sup>ts</sup>*/+; physiology, A307/+;UAS-*shi<sup>ts</sup>*/+.

<sup>†</sup>Pupal stage as % of total duration at 18°C (196 hours), restrictive temperature 30°C.

<sup>‡</sup>Wild type is defined as ≤1 msec and able to follow stimuli one-to-one at 100 Hz.

nd, not determined (the TTM muscle is missing or reduced in size for TS before 50%); TS, temperature shift; n, the number of GFs examined.

<sup>§</sup>Significantly different from the non-TS controls at the 0.05 level.

**Table 2. Retraction and regeneration of the GF**

Stage*			Location of the axon terminal					
Phase	TS begins	Dissection	<i>n</i>	t3 (%)	t2 [bendless (%)]	t1 (%)	Connective (%)	Brain (%)
I	0	After TS	36	0	3 (0)	53	36	8
I	0	Adult	57	46	53 (14)	2	0	0
I	17	After TS	31	0	10 (10)	50	27	13
I	17	Adult	78	27	52 (31)	0	0	18
II	33	Before TS	42	5	90 (0)	5	0	0
II	33	After TS	56	0	36 (32)	64	0	0
II	33	Adult	21	0	86 (52)	0	0	14
II	50	Before TS	10	0	100 (10)	0	0	0
II	50	After TS	65	0	95 (17)	3	0	0
II	50	Adult	58	0	98 (38)	0	0	0
III	67	Before TS	20	5	95 (0)	0	0	0
III	67	After TS	22	5	95 (0)	0	0	0
III	67	Adult	19	5	95 (0)	0	0	0

Genotype: UAS-*lacZ*/+;A307/+;UAS-*shi*<sup>ts</sup>/+ reared at 22°C; restrictive temperature 30°C.

\*Pupal stage as % of total duration at 22°C (144 hours).

TS, temperature shift; t1, first thoracic neuromere; t2, second thoracic neuromere (% of total GFs that do not exhibit a bend); t3, third thoracic neuromere; *n*, the number of GFs examined.

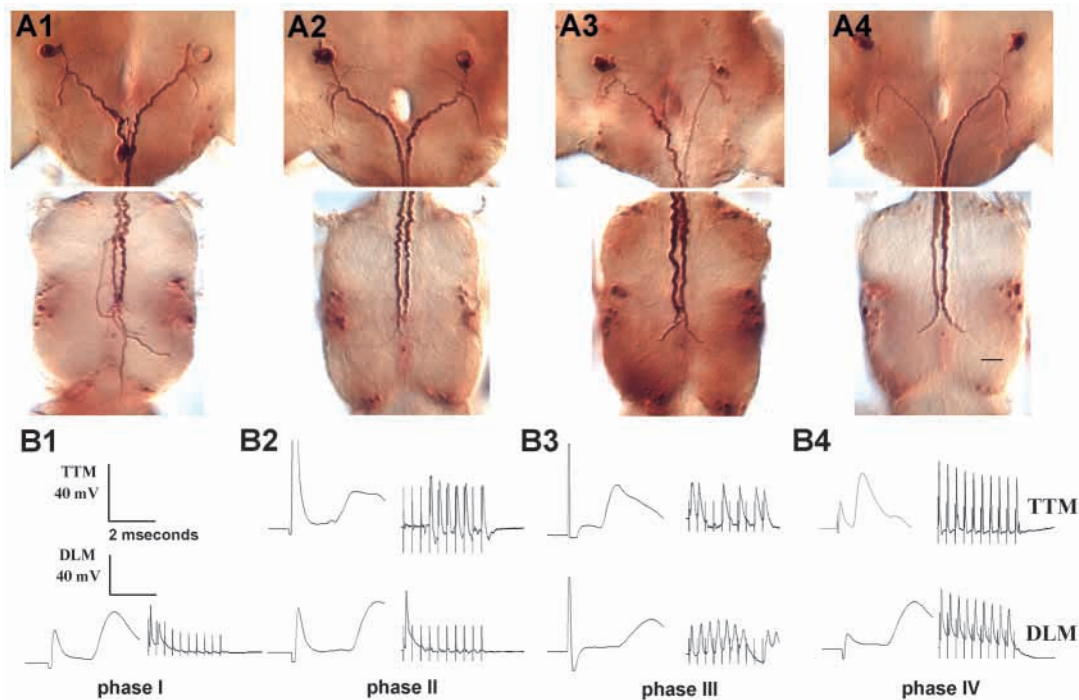


**Fig. 2.** Defects in the adult GF and TTMn are induced by blocking endocytosis at various stages in development. (A) Anatomy of the GF system after various temperature shifts when UAS-*shi*<sup>ts</sup> was driven by the A307 Gal4 enhancer. (A1) A temperature shift at 16% of pupal development followed by regeneration and examination in the adult stage. Two specimens are represented. In one a GF is trapped in the brain, in the thorax of another both GFs exhibit the 'overgrowth' phenotype. (A2) A temperature shift at 33% of pupal development produced a *bendless*-like phenotype where the large lateral bend is missing from both GFs in the adult. (A3) A temperature shift at 75% of development had no detectable effect on the structure of the GF. (A4) Both late temperature shifts and controls exhibit normal bends. This particular specimen was never temperature shifted and illustrates the structure of the GF in the adult stage. Scale bar: 20 μm. (B) Physiology of the GF system. Each pair of traces is taken from a specimen temperature shifted at the time indicated. (B1) Early temperature shifts disrupted the TTM muscle and no recordings could be obtained. The DLM was often excited by the GF but latencies were long and very few stimuli in a train elicit a response. (B2) Temperature shifts during synapse formation increased the latencies and decreased following frequency. (B3) Response latencies were increased and, following frequency, decreased when temperature shifts occurred between 62.5–75% of pupal development. (B4) Temperature shifted at 84% had no statistically significant effect on the physiology and this specimen illustrates the normal physiology (see Table 1 for quantification). In control specimens, the latency for TTM is about 0.9 mseconds and for DLM was 1.4 mseconds; both motoneurons could follow the 100 Hz stimulus without fail. The upper trace in each panel is taken from the TTM, the lower trace from the DLM. In each set of traces, the individual stimulus illustrates the latency and wave form of the response, the sweep with 10 stimuli illustrates the response to repetitive stimuli.

irregularities in shape (Fig. 2A3). However, physiologically, these specimens were defective in the adult, the TTM exhibited long latencies and low following frequencies (Table 1). In brief, during this phase the GF anatomy had stabilized and was resistant to the blockade of endocytosis, while the synapse physiologically was still sensitive to temperature shifts.

#### Phase IV (mature synapse)

Finally, very late temperature shifts (e.g. at 87.5% of pupal development) had no impact on the GFs or their ability to drive the motoneurons.

The anatomy of the GFs was indistinguishable from controls (Fig. 2A4) and functionally there were no significant defects on latency or following frequency for either TTMn or DLMn (Table 1).

## Dynamics of GF retraction and regeneration

### Axon retraction

In order to appreciate the dynamics of the anatomical changes, we used P[Gal4]-A307 to express UAS-*shi<sup>ts</sup>* and examined the axonal phenotypes before the temperature shift, immediately after the temperature shifts as well as at later times (Fig. 3, Table 2). The GF grew into the thorax at the beginning of pupal development (Allen et al., 1998; Phelan et al., 1996) and when dissected immediately after the temperature shift, the GF anatomy could be reliably observed. Most of the GF axons terminated in 'retraction bulb' (Fig. 3A2, arrows) often exhibiting a long slender extension towards the target (Bernstein and Lichtman, 1999). These retraction bulbs were located in the connective (36% of the GFs) or the first thoracic neuromere (53% of the GFs) and a minority terminated in the

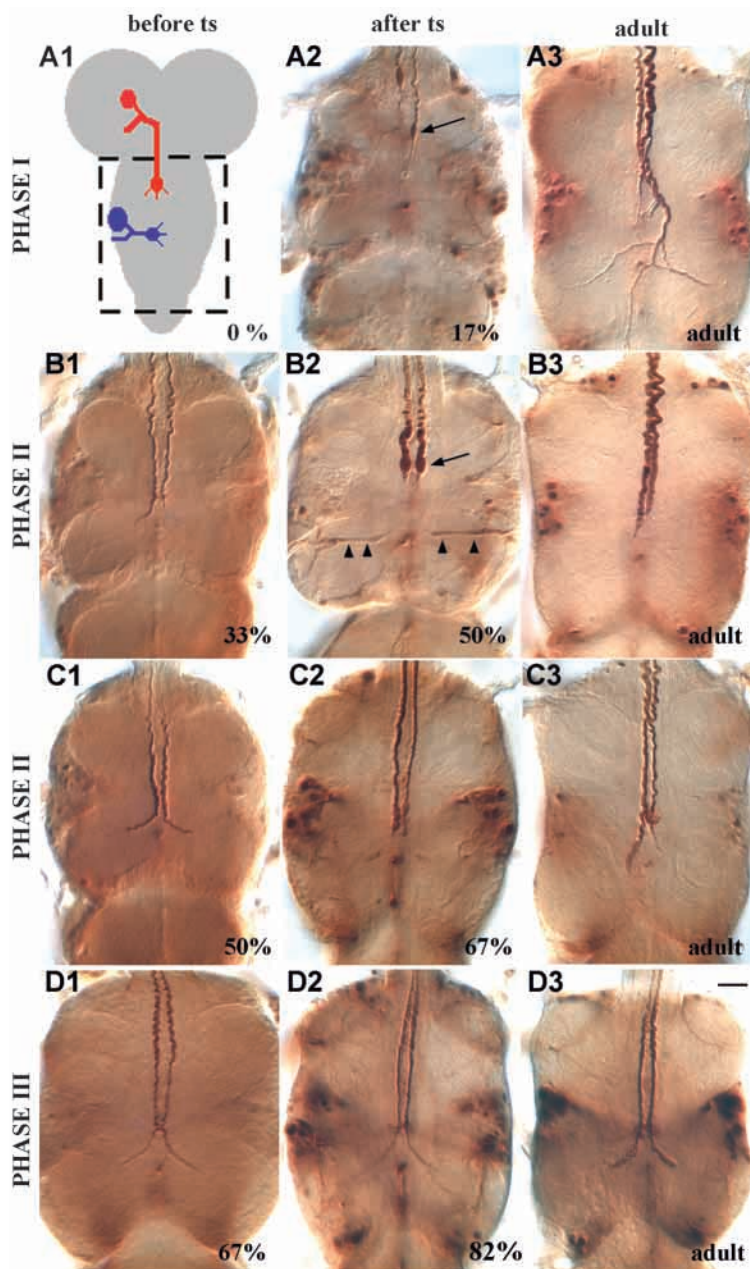


**Fig. 3.** The dynamics of axon retraction and regeneration. Each row represents the results for a temperature shift initiated at the time indicated. Each column represents the structure at a different time with respect to the temperature shift. The left column shows examples immediately before the temperature shift, the middle column immediately after the temperature shift and the right column illustrates the adult CNS after the temperature shift. (A) Temperature shift initiated at the beginning of pupariation (P0). (A1) Schematic version of the GF at P0. The GF has not reached the target area in the early phase of growth and the axons are very thin, making it difficult to stain and visualize with our methods. The schematic illustrates the approximate location of the axons at this time as well as showing the portion of the CNS represented in all the panels (dashed box). (A2) The axons at the end of a temperature shift that began at pupariation. Both axons have retracted into the anterior end of the thorax and each exhibits a retraction bulb (arrow) near the terminal and a thin retraction tail extending toward the target. (A3) Overgrowth of the axon in the adult after regeneration at the permissive temperature. (B) Temperature shift initiated at 33% of pupal development (Phase II). (B1) The structure of the GF at 33% of development. Most specimens exhibited the laterally projecting terminal illustrated by the left GF, a minority of GFs have just begun to make the bend as seen for the right GF. (B2) Dissection at the end of the temperature shift (50%) shows that both axon terminals have retracted into the first thoracic neuromere and terminate in retraction bulbs (arrow). In this specimen the dendrites of the TTMn were also visible (arrowheads) indicating the extent of the GF retraction. The dendrites of the TTMn appeared normal in this specimen. (B3) After regeneration, both GFs tapered to an end in the target area and neither showed the laterally projecting terminal. (C) Temperature shift initiated at 50% of pupal development. (C1) Both GFs exhibited the normal lateral extension of the presynaptic terminal at 50% of pupal development. (C2) Retraction of the presynaptic terminal immediately after a temperature shift. Note that the presynaptic terminal has withdrawn but the axon did not retract away from the target area. (C3) The adult regenerated axon. In this case a large swollen region was present on the right GF just anterior to the presynaptic terminal. (D) Temperature shift initiated at 66% of pupal development. (D1) The GF structure at 66% of pupal development exhibited normal lateral extensions. (D2) Immediately after a temperature shift, there was no obvious defect. (D3) An adult specimen indistinguishable from controls. Genotype of all specimens; UAS-*lacZ*/+;A307/+;UAS-*shi<sup>ts</sup>*/+. Scale bar: 20  $\mu$ m.

brain (Table 2). By contrast, GFs treated in the same way but examined as adults exhibit overgrowth (Fig. 3A3) and the terminals were located in the second thoracic neuromere (53% of the GFs) and often extended to the third thoracic neuromere (46% of the GFs), demonstrating regeneration of the axons after return to the permissive temperature. When the axon was examined at various stages after the temperature shift axon growth recovered and the overgrowth phenotype was detected as soon as 48 hours after the temperature shift ended (at 75% of pupal development). This suggested that the regenerating axons exhibited the overgrowth defect as soon as they reached the target region.

### Synapse retraction

When the temperature shift was initiated at 33% of pupal development and the GF was examined immediately after the shift approximately two thirds of the axons (64%) terminated in retraction bulbs. These retraction bulbs were located either in the first or second thoracic neuromere, none retracted into the connective or brain (Table 2). In some specimens the retraction bulbs exhibited single long extensions that resembled 'retraction tails' that reached the target area (Fig. 3B). In occasional specimens the expression in the TTMn was strong enough to reveal the structure of the GF and TTMn simultaneously and the separation between the GF and the dendrites of TTMn was clear (Fig. 3B2, arrowheads). In control specimens for this genotype, all of the GFs had reached the target area by 33% and most exhibited the characteristic

bend, albeit smaller and thinner than in adults (Fig. 3B1, Table 2). These observations suggested that the axons had reached the target area and often elaborated incipient presynaptic terminals, which were then retracted during the temperature shift. When specimens were allowed to mature to the adult stage after the temperature shift the axons usually regenerated to the target area but the lateral bend along the TTMn dendrite, was missing and the axon tapered to an end in the target region (Fig. 3B3, adult). Apparently, the inability to form a functional synapse after the temperature shift was not due to a defect in axonal growth, as the axon was able to regenerate into the target area, but rather to a defect in synapse formation.

At 50% of pupal development the GF is known to be dye-coupled to a number of its targets, including the TTMn (Jacobs et al., 2000; Phelan et al., 1996), and the presynaptic terminal is beginning to take on the adult appearance. Temperature shifts at this stage exhibited less dramatic retraction and immediately after the temperature shift the presynaptic terminal had retracted only slightly from the target area (Fig. 3C2). The defect developed progressively and more GFs were anatomically defective in the adults than immediately after the temperature shift (Table 2). When examined in the adult stage the presynaptic terminal had expanded but there were often defects in its structure and the bend was not as large as in control specimens (Fig. 3C3). The synapse retraction was more complete if the temperature shift was longer in duration (48 hours rather than 24 hours, data not shown). These results demonstrated that this immature synapse could be retracted

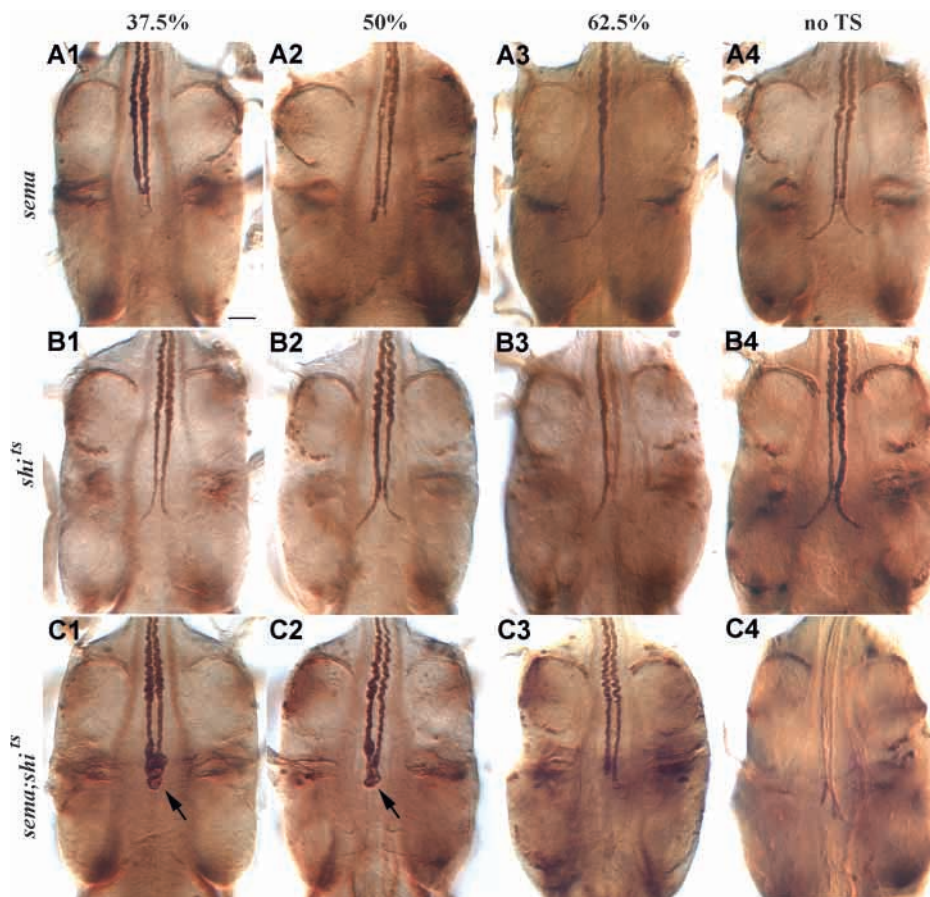


**Fig. 4.** Interactions between *shits* and *semala*. Each row illustrates the results for a different UAS-construct, driven by *c17*. Each column indicates the results for a temperature shift at the indicated time. All specimens were dissected in the adult stage. (A) Specimens expressing UAS-*semala* alone. (A1,A2) Temperature shifts during synapse formation caused *bendless*-like phenotypes. (A3) Late temperature shifts (62.5% of pupal development) had no effect and were indistinguishable from (A4) controls that were not temperature shifted. (B) Specimens expressing only UAS-*shits*. Very few defects were observed, usually all axons reached the target area and extended a lateral bend independent of the temperature shift. (C) UAS-*semala* and UAS-*shits* were targeted to the presynaptic GFs. (C1) When temperature shifted at 37.5% of pupal development GFs exhibited a swollen terminal filled with vesicles in the target area (arrow). (C2) The left GF in this example at 50% of pupal development exhibits a swollen terminal and a retraction tail, the right GF is dramatically swollen and filled with membrane bound vesicles (arrow). (C3) Late temperature shifts cause some retraction and few swellings or vesicles. (C4) Control specimen that was not temperature shifted. Scale bar in A1: 20  $\mu$ m.

even after dye-coupling had occurred at 40% (Jacobs et al., 2000) but could usually not be regenerated after the temperature shift.

### Synapse stabilization

Finally, temperature shifts during the final third of pupal development caused minor anatomical defects in the synaptic terminal but no retraction. For example, when exposed to the restrictive temperature beginning at 67% of pupal development and dissected immediately after the temperature shift, the axon extended laterally as it would in wild-type specimens. The terminal was often irregular in shape and contained swellings at various places along the terminal but the laterally directed bend was usually present (Fig. 3D2). When dissected in the adult stage the result was very similar. Most terminals exhibited the lateral bend and approximately half of these synaptic terminals were distorted by swellings in the bend or at a site just anterior to the bend. When the temperature shift was extended to 48 hours, there was no additional synapse retraction indicating that the synapse had stabilized after 67% and could not be retracted from the target area after this stage.

### Controls for the temperature shifts

A variety of controls were carried out to distinguish the effect of blocking endocytosis from non-specific effects of the temperature shift. We temperature shifted specimens carrying the A307 enhancer and the UAS-*lacZ* but no UAS-*shi<sup>ts</sup>* at various times but all GFs appeared wild type. Thus, the temperature shift per se did not cause detectable anatomical defects in GF. To assess the possibility that the UAS-*shi<sup>ts</sup>* construct was 'leaky', we applied temperature shifts to specimens carrying the UAS-*shi<sup>ts</sup>* construct but no Gal4 driver.

All specimens treated in this way exhibited wild-type physiology demonstrating that the UAS-*shi<sup>ts</sup>* construct must be driven by Gal4 in order to have its effects. Finally, we reared specimens carrying the UAS-*shi<sup>ts</sup>* construct and a Gal4 driver without temperature shifts and this led to wild-type anatomy in 90% of the cases (Table 3).

### Interactions between *shibire<sup>ts</sup>* and *semaphorin*

One possible role for endocytosis is the regulation of the residence time of receptors at the surface of the axon terminal. We have shown that *Sema1a* is involved in assembly of the GF system and may serve presynaptically as a repulsive receptor during target recognition or synapse formation (Godenschwege et al., 2002a). To determine the phase of effect of *Sema1a* more precisely and to test the idea that endocytosis regulates the *Sema1a* during assembly of the GF system, we co-expressed UAS-*shi<sup>ts</sup>* and UAS-*sema1a* and then examined the effects of temperature shifts at the time of synapse formation and stabilization (phase II and III). We first determined the effects of UAS-*shi<sup>ts</sup>* and UAS-*sema1a* alone and then compared these with specimens expressing both constructs. In order to simplify the interpretation, we limited the expression to the presynaptic cells through the use of the P[Gal4]-c17 enhancer and focused on phase II when synapse formation occurs.

### Temporal aspects of *Sema1a* function

It is well known that the P[Gal4] enhancers and the UAS-drivers are temperature sensitive and we took advantage of this property to determine the critical periods for *Sema1a*. In specimens (c17/UAS-*sema1a*) reared at 18°C and never temperature shifted most of the axons were normal in structure (83% wild type) and function (67% wild type) similar to that

**Table 3. Interactions between *semaphorin1a* and *shibire<sup>ts</sup>***

Anatomy								Physiology					
Phase	Genotype*	Stage <sup>†</sup> of TS (dissection)	<i>n</i>	Wild type (%)	Bendless <sup>‡</sup> (vesicles) (%)	t1 (%)	Brain (%)	<i>n</i>	TTM wild type <sup>§</sup> (%)	TTM latency in mseconds	TTM FF (%)	TTM dis- connection (%)	TTM or DLM connection (%)
I	shi <sup>ts</sup>	12.5 (adult)	25	88	8	0	4	11	81	1.05	90.7	0	100
I	sema	12.5 (adult)	31	58	26	13	3	19	33	1.14 <sup>¶</sup>	58 <sup>¶</sup>	5	100
II	shi <sup>ts</sup>	37.5 (adult)	32	94	6	0	0	16	88	1.01	91.3	0	100
II	sema1a	37.5 (adult)	13	15	73	12	0	12	0	1.67 <sup>¶</sup>	30.4 <sup>¶</sup>	8	92
II	shi <sup>ts</sup> +sema	37.5 (adult)	18	6	44 (44)	6	44	13	0	1.61 <sup>¶</sup>	14.9 <sup>¶</sup>	46	54
II	shi <sup>ts</sup> +sema	37.5 (after TS)	33	0	46 (0)	23	31	nd	nd	nd	nd	nd	nd
II	shi <sup>ts</sup>	50 (adult)	36	83	17	0	0	16	56	1.09	79 <sup>¶</sup>	0	100
II	sema	50 (adult)	26	38	62	0	0	14	7	1.18 <sup>¶</sup>	54.8 <sup>¶</sup>	7	93
II	shi <sup>ts</sup> +sema	50 (adult)	29	21	59 (24)	7	14	17	0	1.59 <sup>¶</sup>	42.6 <sup>¶</sup>	35	82
II	shi <sup>ts</sup> +sema	50 (after TS)	11	0	55 (0)	27	18	nd	nd	nd	nd	nd	nd
III	shi <sup>ts</sup>	62.5 (adult)	19	95	5	0	0	18	44	1.08	95.9	0	100
III	sema	62.5 (adult)	18	83	17	0	0	19	58	1.03	83.6	5	95
III	shi <sup>ts</sup> +sema	62.5 (adult)	18	33	61 (17)	0	6	14	0	1.85 <sup>¶</sup>	10.9	21	93
III	shi <sup>ts</sup> +sema	62.5 (after TS)	21	0	33 (0)	0	14	nd	nd	nd	nd	nd	nd
	shi <sup>ts</sup>	No TS (adult)	31	90	10	0	0	21	90	0.92	99.8	0	100
	sema	No TS (adult)	18	83	11	6	0	21	67	0.96	81.3	5	100
	shi <sup>ts</sup> +sema	No TS (adult)	58	50	40	5	5	22	45	1.08	74.2	0	100

\*Genotype: anatomy, c17,UAS-*lacZ* crossed to UAS-*shi<sup>ts</sup>* or UAS-*sema1a* or UAS-*shi<sup>ts</sup>*,UAS-*sema1a*; physiology, c17 crossed to UAS-*shi<sup>ts</sup>* or UAS-*sema1a* or UAS-*shi<sup>ts</sup>*,UAS-*sema1a*.

†Stage as percent of pupal development reared at 18°C; restrictive temperature 30°C.

‡Percentages of total GFs that reach the second thoracic neuromere but do not exhibit a bend (% of total GFs that reach the second thoracic neuromere and exhibit large vesicles in the axon terminal).

§Wild type is defined as ≤1 msecond and able to follow stimuli one-to-one at 100 Hz.

TS, temperature shift; t1, first thoracic neuromere; *n*, the number of GFs examined.

¶Significantly different from controls ( $P<0.05$ ).

seen for specimens reared at 22°C (Godenschwege et al., 2002a). When specimens were temperature shifted to 30°C during synapse formation (37.5% of pupal development), the axon terminal typically lacked the bend in adult flies and physiologically all GF-to-TTMn contacts exhibited long latencies and/or low following frequencies (Fig. 4A1, Table 3). When the temperature shift occurred at 50% of pupal development, a minority were anatomically wild type and a few were physiologically normal (Table 3, Fig. 4A2). By contrast, temperature shifts before or after these times had only minor effects in comparison to non-temperature-shifted control specimens (Table 3). These results confirmed that *Sema1a* was disruptive for synapse formation and suggested that it must be removed in order for synapse formation to proceed normally. In addition, these new results demonstrated a critical period for removal of *Sema1a* during the period of synapse formation and showed that its acute presence during phase II had a permanent effect that prevented regeneration of a functional synapse.

#### Weak effects when *shi<sup>ts</sup>* is expressed at low levels

When UAS-*shi<sup>ts</sup>* alone was driven by *c17*, the specimens temperature shifted at different times and the GF examined in the adults (Fig. 4B) the results parallel those for A307 but the defects were much weaker. Specimens temperature shifted during synapse formation (e.g. 50% stage of pupal development) occasionally resulted in a *bendless*-like phenotype (17%) and physiologically a slightly disrupted GF-TTMn connection (44% of the specimens, Table 3). Late temperature shifts (at 62.5% of pupal development) were anatomically indistinguishable from the controls and physiologically weakly affected. In summary, expression of UAS-*shi<sup>ts</sup>* with the *c17* driver has mild effects on the GF anatomically and physiologically, enabling us to study the interaction of *shibire<sup>ts</sup>* with *sema1a*.

#### Co-expression of UAS-*sema* and UAS-*shi<sup>ts</sup>*

In order to determine whether *Sema1a* trafficking/signaling was dependent on endocytosis, we used P[Gal4]-*c17* to co-express UAS-*shi<sup>ts</sup>* and UAS-*sema1a* and searched for interactions. It was clear that even without a shift to the restrictive temperature, there was an interaction, because only half of the specimens exhibited anatomically normal GFs and the remainder were *bendless*-like or did not reach the target area (Table 3). This suggested that both constructs were expressed at low levels at 18°C and indicated that UAS-*shi<sup>ts</sup>* was having an effect even at the permissive temperature of 18°C, an effect that was detected in double mutant specimens but not when UAS-*shi<sup>ts</sup>* was expressed alone. The physiology was correlated with this as approximately half were wild type and half were mutant (Table 3).

Temperature shifts during the period of synapse formation (phase II) caused dramatic defects in the presynaptic terminal (Table 3). When UAS-*sema1a* and UAS-*shi<sup>ts</sup>* were co-expressed and the temperature shifted at 37.5% of pupal development, nearly all GFs were defective; approximately half (44%) of the GFs terminated in the thorax and were anatomically defective (Fig. 4C1) and most of the remaining axons terminated in the brain (Table 3). When the temperature shift began at 50% of pupal development, most axons exited the brain but the presynaptic terminals in the thorax were

defective (Fig. 4C2, Table 3). The disrupted axon terminals were unusually large, and often filled with membrane-bound vesicles that excluded *lacZ* (Fig. 4C1 and Fig. 4C2). Small vesicles were occasionally observed when either construct was expressed alone (data not shown) but the large vesicles in the co-expression experiment highlight the possibility that membrane trafficking has been disrupted when both constructs were expressed. The physiological results were consistent with these anatomical findings. Although the axon terminals were connected to one or the other motoneurons, all connections were physiologically defective (Table 3). Finally, the results also show that the defect is a progressive degenerative effect as these large vesicular structures only emerge after a delay. The large vesicles were never seen immediately after the temperature shift and were only seen in adults after temperature shifts at 33% or 50% of pupal development (Table 3).

Finally, the interaction of *shibire<sup>ts</sup>* and *sema1a* was further supported by temperature shifts that began at 62.5% of pupal development (phase III). When *sema1a* and *shi<sup>ts</sup>* were co-expressed by the weak *c17* driver and temperature shifted at this pupal developmental stage, none of the specimens exhibited a bend when dissected directly after the temperature shift, suggesting all immature synapses had retracted (Table 3). A few GFs were able to regenerate anatomically after the temperature shift but physiologically, not a single fully functional giant synapse was restored (Table 3). A temperature shift in phase III was not able to induce the retraction of the giant synapse when UAS-*shi<sup>ts</sup>* was driven with the strong driver A307 and only minor effects on the GF anatomy were seen when either construct was expressed alone with *c17* and temperature shifted. These findings demonstrate that *sema1a* and *shibire<sup>ts</sup>* have a synergistically enhanced ability to induce the retraction of a synapse. In summary, comparison of the co-expression experiments with those for either UAS-*shi<sup>ts</sup>* alone or UAS-*sema1a* alone supports the idea that the two are interacting and suggests a role for membrane trafficking in *Sema1a* signaling.

## DISCUSSION

Blocking endocytosis seems on first examination to be a relatively blunt instrument for the analysis of nervous system development because of the wide variety of functions it might disrupt. However, two distinct effects have helped dissect pupal development of the GF system. First, blocking endocytosis caused retraction and subsequent regeneration of the GF, which altered the timing of axon growth and disrupted the resulting structure and function. This allowed us to define four phases in development of the giant fiber system. Second, a role for membrane trafficking was highlighted by an interaction between *sema1a* and *shibire<sup>ts</sup>*, which created large vesicles in the axon terminal. Blocking endocytosis at the time of synapse formation appeared to enhance the disruptive effect of *Sema1a* on synapse formation. This supported the idea that *Sema1a*, in its role as a repulsive receptor, must be removed from the growth cone during synaptogenesis (Godenschwege et al., 2002a). The interaction with *shibire<sup>ts</sup>* suggested that this was likely to be regulated by dynamin-dependent endocytosis

#### Four phases of circuit assembly revealed by heterochronic growth

In the present experiments, targeted blockade of endocytosis had direct effects on axon growth and retraction, presumably by disrupting the recycling of membrane in a rapidly growing axon terminal (Diefenbach et al., 1999). Previously, neurons from mutant *shi<sup>ts1</sup>* animals were grown in culture and a shift to the restrictive temperature caused collapse of growth cones, cessation of axon outgrowth and axon retraction. Shifting back to the permissive temperature led to a resumption of growth and a rebound of growth rate (Kim and Wu, 1987). The temperatures used and the temperature shift paradigms employed in vitro were identical to those we used to assay the timing of developmental events of the giant fiber in vivo. When we challenged the GF at various times during pupal development by blocking endocytosis, we identified four phases in the GF development: an early pathfinding phase, an intermediate phase of synaptogenesis, a late stabilization process and, finally, a mature synapse.

When we blocked endocytosis during pathfinding; the axons retracted during the temperature shift and when returned to the permissive temperature regenerated and overgrew the target area (phase I, Fig. 1A). By contrast, temperature shifts which correspond to the time that the GF is being transformed from growth cone to synapse (phase II) produced a different effect. GFs retracted but when examined as adults the axons did not overgrow the target area but rather stopped in the target area and lacked the lateral bends. The initial effects induced by blocking endocytosis during both, phase I and II, were likely to be caused by the retraction of the axon and the subsequent heterochronic growth of the GF. However, the difference of the responses (overgrowth versus *bendless*-like) between phase I and II cannot be attributed directly to the block of endocytosis, but are more likely to be attributed to the different developmental states of the GF when heterochronic regeneration occurred. One relevant difference may be that in phase I most GFs have not contacted the target area and in phase II most GFs have contacted the targets. This means that the heterochronic growth induced in phase I results in naïve GFs that approach the target area with a delay, while heterochronic growth in phase II results in the re-generation of 'experienced' GFs. Possibly the GF loses its ability to regenerate the GF-TTMn synapse after it has contacted the target resulting in the *bendless*-like phenotype.

Finally, blockade of endocytosis in phase III revealed a distinct defect. The function of the synapse was disrupted by temperature shifts although the structure remained normal. This distinguished a stabilized synapse from a mature synapse. Possibly the block of endocytosis during phase III disrupts trafficking of receptors/ligands that are involved in maturation of the giant synapse. For example, Fasciclin 2 and Wingless/Frazzled have been shown to be required for maturation of the neuromuscular junction and correct dynamin-dependent trafficking is required for normal synaptogenesis (Davis et al., 1996; Packard et al., 2002; Schuster et al., 1996).

#### Critical periods for Sema1a function

We have previously suggested that Sema1a must be removed from the presynaptic terminal in order for synaptogenesis to proceed correctly, but the exact timing and mechanism for

these events were not examined (Godenschwege et al., 2002a). In the present report, we show that the acute presence of Sema1a during synapse formation had a lasting effect that prevented the regeneration of a functional synapse. We examined the temporal aspects of Sema1a function, independent of endocytosis, by taking advantage of the temperature sensitivity of the UAS constructs. Overexpression of Sema1a during synapse formation (phase II) caused the majority of axons to terminate in *bendless*-like structure and exhibit weak synaptic connections (Table 3), while the acute presence of Sema1a in phase I or phase III had only minor effects. This suggests that removal of Sema1a is crucial for synaptogenesis. The sensitivity to Sema1a overexpression overlapped the time that the GF first contacted its targets and becomes dye-coupled to them (Phelan et al., 1996) suggesting that Sema1a plays a role in the transition from growth cone to synapse. Interestingly, the *bendless* mutant causes phenotypes similar to those seen when Sema1a is overexpressed in the present experiments (Thomas and Wyman, 1984). When *bendless* was cloned and shown to be a ubiquitin conjugase the authors speculated that the *bendless* mutant may be affecting the lifetime of Sema1a on the GF growth cone (Muralidhar and Thomas, 1993; Oh et al., 1994). The finding that Sema1a trafficking is involved in the assembly of the GF-TTMn synapse and the recent realization that ubiquitin can function to regulate trafficking of membrane proteins (Murphey and Godenschwege, 2002) suggest that Sema1a trafficking may be regulated by Bendless.

#### Endocytosis and Sema1a signaling

Endocytosis plays an important role in ligand-dependent receptor responses that serve as a mechanism for the regulation of signal strength in a variety of signaling pathways (Di Fiore and De Camilli, 2001; Hicke, 1999). We propose that during the transition from growth cone to synapse, Sema1a, which functions as a receptor on the GF growth cone, encounters its ligand and this slows the progress of the growth cone as a first step in the transition (Godenschwege et al., 2002a). However, the repulsive signaling of Sema1a must be downregulated because it is disruptive for subsequent events in the formation of the synapse and it is therefore normally removed through a dynamin-dependent receptor-mediated endocytosis. When UAS-*sema1a* was combined with UAS-*shibire<sup>ts</sup>* in a genetic interaction experiment, simultaneous overexpression of Sema1a and the block of endocytosis exaggerated the disruptive effects of Sema1a. One effect was greater retraction of the axon presumably by enhancing the total amount of the repulsive receptor (Sema1a) present on the surface of the presynaptic cell (Table 3). A second effect was the accumulation of large vesicles in the axon terminal. Our interpretation is that the unusually high levels of Sema1a at the surface activated excessive receptor-mediated endocytosis. This may cause a vesicular 'traffic jam' in the growth cone, thereby disrupting the ability to carry out normal functions. These vesicular traffic jams are consistent with other experiments on the GF system that show similar phenotypes. For example, blocking retrograde transport by expression of a truncated version of the P150<sup>Glued</sup> component of the dynein-dynactin motor also caused the formation of large vesicles in the GF terminal (Allen et al., 1999). Although we cannot directly link the vesicles seen in these various genotypes to

each other, the common phenotype makes it seem likely that we are interrupting a common membrane trafficking pathway involved in synapse formation. Markers for various aspects of the endosomal system in *Drosophila* (Sweeney and Davis, 2002) will eventually allow us to identify the origin of these vesicles and link the various genotypes together in a model of receptor trafficking and synapse formation.

In vertebrate neurons, semaphorin signaling has been linked to endocytosis during growth cone guidance and growth cone collapse (Fournier et al., 2000; Journey et al., 2002). Sema3a serves as a ligand for the plexin/neuropilin receptor complex and has been shown to stimulate endocytosis during growth cone collapse. Moreover this is a Rac1-mediated process as Sema3a and Rac1 are associated with vesicles after Sema3a treatment (Fournier et al., 2000) and Rac1 is required for endocytosis of growth cone membrane during growth cone collapse (Journey et al., 2002). Although Sema3a is working as a ligand in vertebrate neurons and Sema1a is working as a receptor in the GF, there are a number of striking parallels between the vertebrate work and the *Drosophila* work. In both cases, semaphorin and endocytosis are linked and in both cases Rac1 is involved in growth cone structure and behavior. We demonstrated elsewhere that overexpression of the small GTPase Rac1 disrupted the termination of the GF and caused the accumulation of large vesicles in the terminal (Allen et al., 2000). Although we did not experimentally link Rac1 to the semaphorin effects, the similarity between the GF phenotypes in these various experiments is consistent with the vertebrate work. The involvement of semaphorins, Rac1 and endocytosis in growth cone repulsion in vertebrate neurons and in the transition to synapse formation in the *Drosophila* GF system highlights the similarities between the systems. As synapse formation requires that growth cones slow or stop as they invade a target region, it seems likely that the growth cone guidance machinery has been commandeered to regulate the initial stages of synaptogenesis.

Surprisingly, the appearance of large vesicles in the GF in the interaction experiment between Sema1a and endocytosis was delayed with respect to the temperature shift as no vesicles were detected immediately after the temperature shift but rather the vesicles emerged as pupal development proceeded (Table 3). There are numerous suggestions that defects in membrane trafficking are linked to neurodegeneration and that these vesicles in the GF may be a prelude to synaptic degeneration; we are exploring this possibility.

This work was supported by NIH grant R01-NS044609.

## REFERENCES

- Allen, M. J., Drummond, J. A. and Moffat, K. G. (1998). Development of the giant fiber neuron of *Drosophila melanogaster*. *J. Comp. Neurol.* **397**, 519-531.
- Allen, M. J., Shan, X., Caruccio, P., Froggett, S. J., Moffat, K. G. and Murphey, R. K. (1999). Targeted expression of truncated glued disrupts giant fiber synapse formation in *Drosophila*. *J. Neurosci.* **19**, 9374-9384.
- Allen, M. J., Shan, X. and Murphey, R. K. (2000). A role for *Drosophila* Drac1 in neurite outgrowth and synaptogenesis in the giant fiber system. *Mol. Cell. Neurosci.* **16**, 754-765.
- Ashburner, M. (1989). *Drosophila*. Cold Spring Harbor, NY: Cold Spring Harbor Laboratory.
- Bainbridge, S. P. and Bownes, M. (1981). Staging the metamorphosis of *Drosophila melanogaster*. *J. Embryol. Exp. Morphol.* **66**, 57-80.
- Bernstein, M. and Lichtman, J. W. (1999). Axonal atrophy: the retraction reaction. *Curr. Opin. Neurobiol.* **9**, 364-370.
- Damke, H., Baba, T., van der Bliek, A. M. and Schmid, S. L. (1995a). Clathrin-independent pinocytosis is induced in cells overexpressing a temperature-sensitive mutant of dynamin. *J. Cell Biol.* **131**, 69-80.
- Damke, H., Gossen, M., Freundlieb, S., Bujard, H. and Schmid, S. L. (1995b). Tightly regulated and inducible expression of dominant interfering dynamin mutant in stably transformed HeLa cells. *Methods Enzymol.* **257**, 209-220.
- Davis, G. W., Schuster, C. M. and Goodman, C. S. (1996). Genetic dissection of structural and functional components of synaptic plasticity. III. CREB is necessary for presynaptic functional plasticity. *Neuron* **17**, 669-679.
- Di Fiore, P. P. and De Camilli, P. (2001). Endocytosis and signaling: an inseparable partnership. *Cell* **106**, 1-4.
- Diefenbach, T. J., Guthrie, P. B., Stier, H., Billups, B. and Kater, S. B. (1999). Membrane recycling in the neuronal growth cone revealed by FM1-43 labeling. *J. Neurosci.* **19**, 9436-9444.
- Fournier, A. E., Kalb, R. G. and Strittmatter, S. M. (2000). Rho GTPases and axonal growth cone collapse. *Methods Enzymol.* **325**, 473-482.
- Godenschwege, T. A., Hu, H., Shan-Crofts, X., Goodman, C. S. and Murphey, R. K. (2002a). Bi-directional signaling by Semaphorin 1a during central synapse formation in *Drosophila*. *Nat. Neurosci.* **5**, 1294-1301.
- Godenschwege, T. A., Simpson, J. H., Shan, X., Bashaw, G. J., Goodman, C. S. and Murphey, R. K. (2002b). Ectopic expression in the giant fiber system of *Drosophila* reveals distinct roles for roundabout (Robo), Robo2, and Robo3 in dendritic guidance and synaptic connectivity. *J. Neurosci.* **22**, 3117-3129.
- Heerssen, H. M. and Segal, R. A. (2002). Location, location, location: a spatial view of neurotrophin signal transduction. *Trends Neurosci.* **25**, 160-165.
- Hicke, L. (1999). Gettin' down with ubiquitin: turning off cell-surface receptors, transporters and channels. *Trends Cell Biol.* **9**, 107-112.
- Hummon, M. R. and Costello, W. J. (1987). Induced disruption in the connectivity of an identified neuron in the *Drosophila* ts mutant shibire. *J. Neurosci.* **7**, 3633-3638.
- Jacobs, K., Todman, M. G., Allen, M. J., Davies, J. A. and Bacon, J. P. (2000). Synaptogenesis in the giant-fibre system of *Drosophila*: interaction of the giant fibre and its major motoneuronal target. *Development* **127**, 5203-5212.
- Journey, W. M., Gallo, G., Letourneau, P. C. and McLoon, S. C. (2002). Rac1-mediated endocytosis during ephrin-A2- and semaphorin 3A-induced growth cone collapse. *J. Neurosci.* **22**, 6019-6028.
- Kamiguchi, H. and Lemmon, V. (2000). Recycling of the cell adhesion molecule L1 in axonal growth cones. *J. Neurosci.* **20**, 3676-3686.
- Kim, Y. T. and Wu, C. F. (1987). Reversible blockage of neurite development and growth cone formation in neuronal cultures of a temperature-sensitive mutant of *Drosophila*. *J. Neurosci.* **7**, 3245-3255.
- Kitamoto, T. (2001). Conditional modification of behavior in *Drosophila* by targeted expression of a temperature-sensitive shibire allele in defined neurons. *J. Neurobiol.* **47**, 81-92.
- Kitamoto, T. (2002). Conditional disruption of synaptic transmission induces male-male courtship behavior in *Drosophila*. *Proc. Natl. Acad. Sci. USA* **99**, 13232-13237.
- Koenig, J. H. and Ikeda, K. (1996). Synaptic vesicles have two distinct recycling pathways. *J. Cell Biol.* **135**, 797-808.
- Muralidhar, M. G. and Thomas, J. B. (1993). The *Drosophila* bendless gene encodes a neural protein related to ubiquitin-conjugating enzymes. *Neuron* **11**, 253-266.
- Murphey, R. K. and Godenschwege, T. A. (2002). New roles for ubiquitin in the assembly and function of neuronal circuits. *Neuron* **36**, 5-8.
- Oh, C. E., McMahon, R., Benzer, S. and Tanouye, M. A. (1994). bendless, a *Drosophila* gene affecting neuronal connectivity, encodes a ubiquitin-conjugating enzyme homolog. *J. Neurosci.* **14**, 3166-3179.
- Packard, M., Koo, E. S., Gorczyca, M., Sharpe, J., Cumberledge, S. and Budnik, V. (2002). The *Drosophila* Wnt, wingless, provides an essential signal for pre- and postsynaptic differentiation. *Cell* **111**, 319-330.
- Phelan, P., Nakagawa, M., Wilkin, M. B., Moffat, K. G., O'Kane, C. J., Davies, J. A. and Bacon, J. P. (1996). Mutations in shaking-B prevent electrical synapse formation in the *Drosophila* giant fiber system. *J. Neurosci.* **16**, 1101-1113.
- Schuster, C. M., Davis, G. W., Fetter, R. D. and Goodman, C. S. (1996). Genetic dissection of structural and functional components of synaptic plasticity. II. Fasciclin II controls presynaptic structural plasticity. *Neuron* **17**, 655-667.
- Sweeney, S. T. and Davis, G. W. (2002). Unrestricted synaptic growth in

- spinster-a late endosomal protein implicated in TGF-beta-mediated synaptic growth regulation. *Neuron* **36**, 403-416.
- Tanouye, M. A. and Wyman, R. J.** (1980). Motor outputs of giant nerve fiber in *Drosophila*. *J. Neurophysiol.* **44**, 405-421.
- Thomas, J. B. and Wyman, R. J.** (1984). Mutations altering synaptic connectivity between identified neurons in *Drosophila*. *J. Neurosci.* **4**, 530-538.
- Trimarchi, J. R. and Schneiderman, A. M.** (1995). Flight initiations in *Drosophila melanogaster* are mediated by several distinct motor patterns. *J. Comp. Physiol. A* **176**, 355-364.
- van der Bliek, A. M. and Meyerowitz, E. M.** (1991). Dynamin-like protein encoded by the *Drosophila* shibire gene associated with vesicular traffic. *Nature* **351**, 411-414.
- Yu, H. H., Araj, H. H., Ralls, S. A. and Kolodkin, A. L.** (1998). The transmembrane Semaphorin Sema I is required in *Drosophila* for embryonic motor and CNS axon guidance. *Neuron* **20**, 207-220.